AAS 12-225

PRELIMINARY DESIGN OF A HYPERVELOCITY NUCLEAR INTERCEPTOR SYSTEM (HNIS) FOR OPTIMAL DISRUPTION OF NEAR-EARTH OBJECTS

Alan Pitz,* Brian Kaplinger,* and Bong Wie† and David Dearborn‡

When the warning time of an Earth-impacting NEO is short, the use of a nuclear explosive device (NED) may become necessary to optimally disrupt the target NEO in a timely manner. In this situation, a rendezvous mission becomes impractical due to the resulting NEO intercept velocity exceeding 10 km/s. Because the conventional penetrating NEDs require the impact speed to be less than 300 m/s, an innovative concept of blending a hypervelocity kinetic impactor with a subsurface nuclear explosion has been proposed for optimal penetration, fragmentation, and dispersion of the target NEO. A proposed hypervelocity nuclear interceptor system (HNIS) consists of a kinetic-impact leader spacecraft and a follower spacecraft carrying NEDs. This paper describes the conceptual development and design of an HNIS, including thermal shielding of a follower spacecraft, targeting sensors and optical instruments of a leader spacecraft, terminal guidance propulsion systems, and other secondary configurations. Simulations using a hydrodynamic code are conducted to calculate the optimal separation distance between the two vehicles and the thermal and structural limitations encountered by the follower spacecraft carrying NEDs.

INTRODUCTION

Due to uncertainties in asteroid detection and tracking, warning time of an asteroid impact with the Earth can be very short. In the case of an Earth-impacting object ($\approx$ 1 km diameter) discovered without many years of warning, the necessary velocity change becomes very large and the use of high-energy nuclear explosives in space will become inevitable.[1,2,3] The most probable deflection/disruption mission may use a direct intercept trajectory to the target NEO resulting in relative arrival velocities of 10 to 30 km/s.[1] While there are many different nuclear deflection/disruption techniques that can be employed, the subsurface nuclear explosion is most efficient. Delivering nuclear explosives beneath the surface of an NEO proves to be challenging because the conventional penetrating nuclear explosive devices (NED) require the impact speed to be less than 300 m/s.[1] Reference 1 presents the conceptual mission requirements associated with such a mission and an innovative design of a hypervelocity nuclear interceptor system (HNIS) using current technology to execute a nuclear disruption mission with high intercept velocities. A proposed solution includes

*Graduate Research Assistant, Asteroid Deflection Research Center, Iowa State University, 2271 Howe Hall, Room 2355, Ames, IA 50011-2271, alanpitz@gmail.com, bdkaplin@iastate.edu.

†Vance Coffman Endowed Chair Professor, Asteroid Deflection Research Center, 2271 Howe Hall, Room 2355, Ames, IA, 50011-2271, bongwie@iastate.edu.

‡Research physicist/astrophysicist, Lawrence Livermore National Laboratory, 7000 East Avenue, Livermore, CA 94550, working under the auspices of the US Department of Energy at Lawrence Livermore National Laboratory under contract DE-AC52-07NA2734, dearborn2@llnl.gov

a baseline two-body interceptor configuration, thermal shielding of a follower spacecraft, impactor targeting sensors and optical instruments, thruster configurations and terminal guidance phase operations, and other secondary optional configurations. Hydrodynamic simulations are used to asses the mission and to provide thermal and structural design constraints for the follower spacecraft carrying NEDs. Expanding upon system architectures, technologies, and concepts from NASA's Deep Impact, ESA's Don Quijote (canceled), and an Interplanetary Ballistic Missile System (IPBM)[4] studied at the Iowa State Asteroid Deflection Research Center, the preliminary development and design of an HNIS will be discussed in this paper.

NUCLEAR DISRUPTION MISSION REQUIREMENTS

A practical design solution is required for the delivery of a robust and effective subsurface explosion, using available technology, through a direct intercept trajectory, to mitigate the most probable impact threat of NEOs with a short warning time. Since the warning time is short, a rendezvous mission becomes impractical due to the resulting NEO intercept velocity exceeding 10 km/s. NEDs constitute a mature technology, with well-characterized outputs and are the most mass-efficient means for storing energy with today's technology.[1,2,3] Nuclear deflection/disruption strategies to be employed in a last minute, direct intercept mission include standoff explosions, surface contact bursts, and subsurface explosions. For each nuclear technique, accurate timing of the nuclear explosive detonation will be required during the terminal guidance phase of hypervelocity intercept missions. Furthermore, the conventional penetrating NEDs require the impact speed to be less than 300 m/s. A nuclear disruption mission employs nuclear explosives in three different ways. A nuclear standoff explosion is a predetermined height burst and is often considered as the preferred approach among the nuclear options. A second nuclear option exploits a contact burst on the NEO's surface. The most efficient nuclear option involves a subsurface explosion. The subsurface explosion, even with a shallow burial (< 5 m), delivers large energy that can totally fragment the target NEO.[3] The NED payloads are categorized into three classes as:[4] i) a 300-kg NED with a yield of about 300 kt, ii) a 1,000-kg NED with a yield of about 1 Mt, and iii) a 1,500-kg NED with a yield of about 2 Mt.

The nuclear standoff burst technique can be used for long-term warning times. The nuclear standoff scenario utilizes the short burst of energy from a nuclear explosive to heat a thin layer of an NEO's surface. As this layer accelerates away from the NEO, its main body recoils in the opposite direction, thus altering it's trajectory.[2] The area of the NEO's surface that is heated by a standoff nuclear explosion depends on the distance between the asteroid and the point of detonation. Also, the depth of penetration depends on the distance between the surface and the detonation point. Thus, detonation close to the surface heats only a small area close to the explosion. At larger distances, the explosion spreads its energy over a larger area of the asteroid, increasing the angle of effect. As a result of this, the penetration depth decreases. One advantage of this technique is that it does not require stringent spacecraft maneuvers as might be required for a surface or subsurface explosion.

Numerous studies have been conducted in the past to understand the effect of a standoff nuclear explosion and its ΔV capability. In Reference 2, the study simulated the effect of a nuclear standoff detonation on homogeneous 1 km-diameter NEOs with densities between 1.91 and 1.31 g/cm^3. Approximately 40 seconds after the standoff burst, at 150 m above the NEO's surface, the NEO's speed change ranged from 2.2 to 2.4 cm/s. It was estimated that 97.5% of each NEO from all simulations remained intact, while about 2.5% of its mass was ejected at greater than escape speed by the rebound to the shock wave that passes through the body in reaction to the ejection of heated material.[2]

The NEO was held by gravity only and had no tensile strength model. The study concludes that deeper neutron penetration is not dependent on NEO composition.

Another nuclear technique involves the subsurface use of nuclear explosives. The nuclear subsurface method even with a shallow burial (< 5 m) delivers large energy, potentially disrupting the NEO completely.[3] The major advantage of a nuclear subsurface explosion over a surface or aboveground nuclear explosion is the effectiveness with which energy is transmitted into the NEO. The effectiveness of earth-penetrating weapons can be used to illustrate the nuclear subsurface method on an NEO.

Nuclear earth-penetrator weapons (EPWs)[5] with a depth of penetration of approximately 3 meters captures most of the advantage associated with the coupling of ground shock. According to Reference 5, the yield required of a nuclear weapon to destroy a deeply buried target is reduced by a factor of 15 to 25 by ground-shock coupling enhancement. The EPW is designed to detonate below the ground surface after surviving the extremely high shock and structural loading environments that result during high-speed impact and penetration. However, its impact speed is limited to approximately 300 m/s. While additional depth of penetration increases ground-shock coupling, it also increases the uncertainty of EPW survival. The ground-shock coupling factor makes the subsurface technique much more efficient than the other nuclear techniques. The ground-shock coupled energy of an EPW approaches 50% with increasing depth of burst (DOB), and is fully coupled at a scaled DOB of about (2.3)DOB/$Y^{1/3}$, where DOB is the depth of burst in meters and Y is the yield in kilotons.[5] Scaled DOB, defined as DOB/$Y^{1/3}$, is a normalization of the actual depth (or height) of a burst based on weapon yield to that for a 1-kt weapon. Thus, the scaled DOB and actual DOB are the same for a 1-kt EPW. For example, a 1-kt weapon buried 3 meters has a 3 scaled DOB, whereas a 300-kt weapon buried at the same depth of 3 meters couples its energy to the ground as if it were a 1-kt weapon buried at an actual depth of about 0.45 meter; that is, $3/300^{1/3} = 3/6.67 = 0.45$. For a generic 300-kt EPW at 3-m depth of burst (scaled DOB $= 3/(300)^{1/3} = 0.45$), the ground-shock-coupling factor is about 20, which is equivalent to a contact burst of about 6-Mt EPW.

Fundamental principles of Keplerian orbital dynamics can be effectively used for examining the effects of the nuclear subsurface explosion under various physical modeling uncertainties.[3] In Reference 3, the study considers such a nuclear subsurface explosion with a shallow burial of approximately 5 m for different models of NEOs. Sourcing energies equivalent to 900 and 300 kt are used to simulate realistic subsurface explosions.[6] In the simulations, the energy source region expands creating a shock that propagates through the body resulting in fragmentation and dispersal. While the material representations used have been tested in a terrestrial environment, there are low-density objects, like Mathilde, where crater evidence suggests a very porous regolith with efficient shock dissipation.[3,6] Shock propagation may be less efficient in porous material, generally reducing the net impulse from a given amount of energy coupled into the surface.

A common concern for such a powerful nuclear option is the risk that the nuclear disruption mission could result in fragmentation of the NEO, which could substantially increase the damage upon its Earth impact. For short warning time missions, the impact mass can be reduced to 0.2% of the initial mass of the NEO, if the intercept disruption occurs nearly perpendicular to the NEO's orbital flight direction.[3,6,7] Such a sideways push is known to be optimal when a target NEO is in the last orbit before the impact.[6] The mass of Earth-impacting fragments can be further reduced by increasing the intercept-to-impact time or by increasing the nuclear yield. However, disruption/fragmentation is a feasible strategy only if it can be shown that the hazard is truly diminished. Additional research has been recommended, particularly including experiments on real comets and

asteroids, to prove that nuclear disruption can be a valid method.[2]

STATE-OF-THE-ART INTERCEPTOR TECHNOLOGY

Current technology and spacecraft concepts from previous NEO missions provide a starting point for the preliminary design of a baseline HNIS. After the success of previous fly-by missions to comets such as Stardust, NASA developed the Deep Impact mission to achieve a hypervelocity intercept of a comet, retrieve information on the impact event, and obtain several high resolution images of the comet's interior. The Deep Impact mission employed two spacecraft to study the characteristics of the comet Tempel 1. ESA's Don Quijote mission concept also required two spacecraft to study the effects of a hypervelocity kinetic impactor hitting an asteroid. Unfortunately, the mission was canceled due to mission uncertainty and cost. ADRC's IPBM concept takes a versatile payload option approach to be used for a variety of deflection/disruption missions. These various system architectures are exploited for the preliminary design of a baseline HNIS.

NASA's Deep Impact Mission The Deep Impact mission spacecraft consisted of a flyby scientific observing spacecraft and an impactor spacecraft.[8] The flyby and impactor spacecraft were held together to form one spacecraft until the beginning of the terminal guidance phase. During the terminal phase operation, the flyby spacecraft was separated from the impactor to observe the impact event. The flyby spacecraft is equipped with two scientific instruments that serve two main purposes. In the initial stages of the mission, the instruments are used to guide the impactor and the flyby spacecraft towards the target comet, Tempel 1. The two instruments on the flyby spacecraft are the High Resolution Instrument (HRI) and the Medium Resolution Instrument (MRI). To protect these important instruments from the debris in the comet tail and the impact ejecta, the flyby spacecraft rotates and is protected by a Whipple Shield.[8] A Whipple shield is composed of a thin outer bumper that is placed on the outer walls of the spacecraft. The impactor spacecraft of the Deep Impact mission separates approximately 24 hours prior to the impact event and has a relative velocity of approximately 10.2 km/s. The 1-m diameter and 1-m long 370-kg impactor delivered approximately 19 GJ of kinetic energy to create a large crater approximately 100-m wide and 30-m deep.[8] With the help of a shield composed of spherical-shaped copper plates with a mass of 113 kg, the impactor is capable of making a significant crater in the comet for scientific observations. While the Deep Impact mission involved intercepting a comet and observing the comet's nucleus, the mission's purpose was not related to determining the effects of a kinetic impactor impacting the target body.

ESA's Don Quijote Mission Concept The ESA's Don Quijote mission was a previously proposed mission concept with a goal to demonstrate and validate the kinetic impactor's capability of deflecting an asteroid. The first objective was to observe the momentum transfer from the impact by measuring the asteroid's characteristics and also its change in rotation and osculating orbital elements. The second objective is to carry out an Autonomous Surface Package Deployment Engineering eXperiment (ASP-DEX) and perform a mapping of the asteroid. The Don Quijote mission was designed to include two different spacecraft, an orbiter spacecraft called Sancho, and an interceptor spacecraft called Hidalgo. The 491-kg (395-kg dry mass) orbiter spacecraft, Sancho, was going to employ a reconfigured SMART-1 satellite bus. SMART-1 is a 1 cubic meter ESA satellite that orbited around the moon and took high-resolution images of the moon's surface.[9] However, changes had to be made to the communication and power systems of the SMART-1 bus to meet the mission requirements. The Sancho orbiter would be launched into space using a Vega rocket with a Star-48 upper stage. Sancho would arrive at the target NEO and observe the asteroid and its char-

acteristics. The 1,694-kg (532-kg dry mass) Hildago spacecraft launches separately and has been designed to have no moving solar arrays in order to obtain the precise attitude and maneuvering requirements to impact the asteroid. Hidalgo uses advanced on-board computers and a high resolution camera to guide it to the NEO. Hidalgo intercepts the asteroid with a speed of approximately 10 km/s while Sancho deploys the ASP-DEX onto the asteroid.[10] The ASP-DEX obtains information about the asteroid's changes in trajectory, rotation, and physical characteristics.

DESIGN AND ANALYSIS OF A BASELINE HNIS ARCHITECTURE

A Baseline HNIS Mission Architecture

A baseline system concept has been developed to accommodate the technically challenging aspects of the penetrating subsurface nuclear explosion approach. A baseline HNIS consists of a leader spacecraft (kinetic impactor) and a follower spacecraft carrying an NED for the most effective disruption of a target NEO. The leader spacecraft impacts first and creates a shallow crater in the NEO. Then, the follower spacecraft enters the crater and detonates the NED. This baseline HNIS mission concept is illustrated in Figure 1, and the HNIS configurations are also shown in Figures 2a and 2b .

The primary HNIS carrying a 1000-kg NED payload is delivered by a Delta IV M class launch vehicle. The launch vehicle places the HNIS into a direct transfer orbit towards the target NEO. During the transfer phase, the HNIS remains as a single spacecraft by way of the leader staying attached to the follower spacecraft. The HNIS uses a bi-propellant system with a 4,400 N gimbaled engine to execute trajectory correction maneuvers (TCMs). The single spacecraft can be placed in a dormant state, periodically relaying status updates while in transit until the terminal guidance phase.

The terminal phase starts 24 hours before the impact event. Instruments located on the spacecraft detect the target NEO and the subsystems on-board the HNIS become active. Separation occurs between the leader spacecraft and the follower spacecraft and communication is established between the two bodies. Measurements are continued through optical cameras and laser radars located on the leader spacecraft and an intercept location is identified on the asteroid body. The high resolution optical cameras, provides successive images of the NEO to each flight computer where guidance and navigation algorithms are used to guide the impactor and the follower to the intercept location. The computer then uses these calculations to compute the necessary adjustments and instructs the divert and attitude control system to execute a few TCMs. As the distance between the follower spacecraft and NEO becomes smaller, the fuzing system starts, arming the NED payload.

The nuclear fuzing mechanism is initiated by the instruments and the guidance parameters provided by the leader spacecraft (time-to-go, range distance, and range rate). For the subsurface disruption technique, the timing fuze and proximity or radar fuze become armed. The NED is armed prior to the last few minutes of the impact event. A shallow crater is then created as the leader spacecraft hits the NEO. Hot ejecta and debris particles result as the leader spacecraft is destroyed at hypervelocity impact. The follower spacecraft is equipped with a thermally resistant, hypervelocity debris shield that protects the NED and triggering system. The shield deforms and melts as it passes through the hot plasma ejecta and the NED detonates before striking the bottom of the shallow crater. In the case that the NED does not detonate as planned, back-up fuzes are used to salvage/detonate the NED. The accuracies of the instruments, flight computer, and fuzing system are key to a successful disruption mission.

Partitioning options between the leader and follower spacecraft to ensure the follower spacecraft

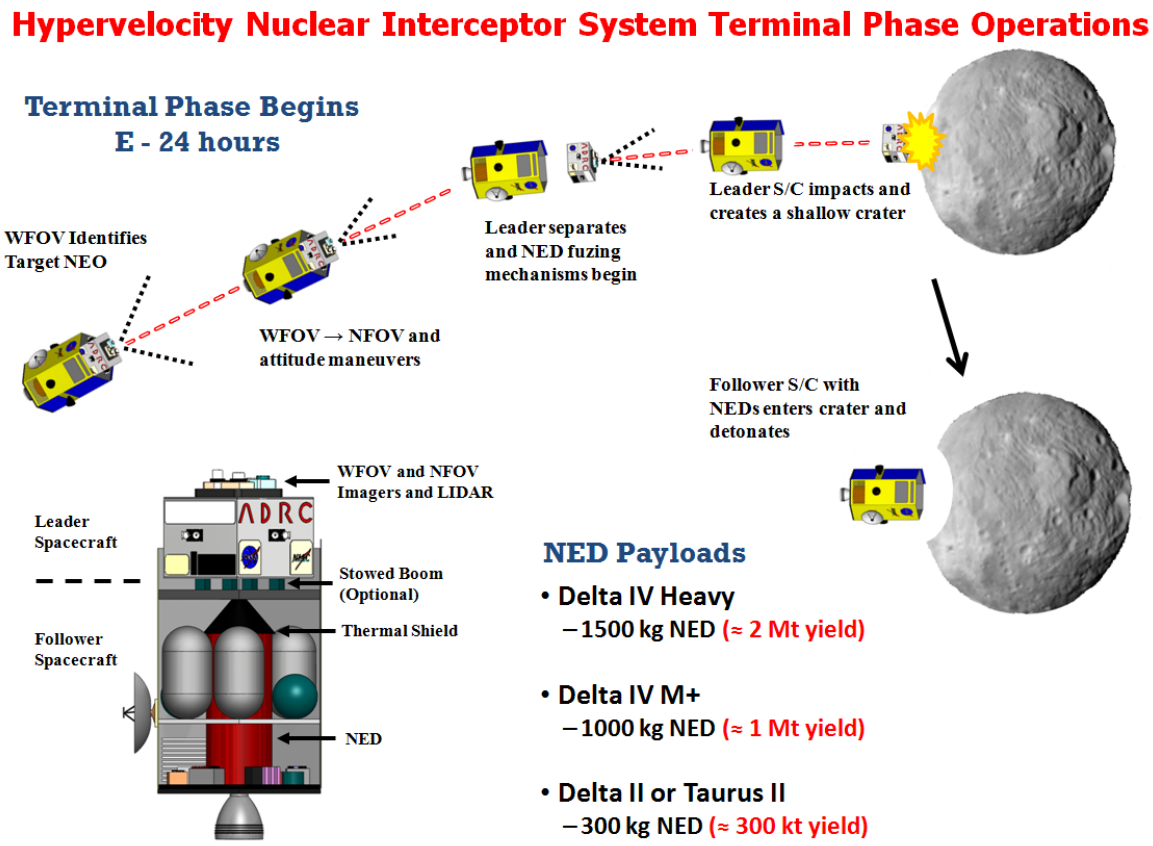

Figure 1: Conceptual illustration of the baseline HNIS mission architecture.

enters the crater opening safely are discussed here. The primary option uses no connection between the two bodies. This configuration depends on the instruments, communication, flight computer, and guidance and tracking algorithms to carryout the terminal phase. Another option includes the use of a rigid connection between the two bodies through deployable booms. Figure 2c shows the primary HNIS with 4 deployable booms. As the booms are deployed and separation distance increases, the center of mass moves from the center towards the front of the follower spacecraft. This new configuration is still treated as a single body but achieves a two-body arrangement. Divert thrusters are pre-positioned at the expected new center of mass location to control the new system as a single body. These large divert thrusters can be gimbaled to achieve the desirable thrust directions. This configuration reduces mission complexity and operations, but is limited to the length of the boom. This is proposed as a optional configuration of the primary HNIS, and it needs further detailed trade-off studies.

Nuclear Fuzing Mechanisms

The NED triggering system is the most vital element of the HNIS. In general, a standard fuzing mechanism ensures optimum weapon effectiveness by detecting that the desired conditions for warhead detonation have been met and to provide an appropriate command signal to the firing set to initiate nuclear detonation. Fuzing generally involves devices to detect the location of the warhead

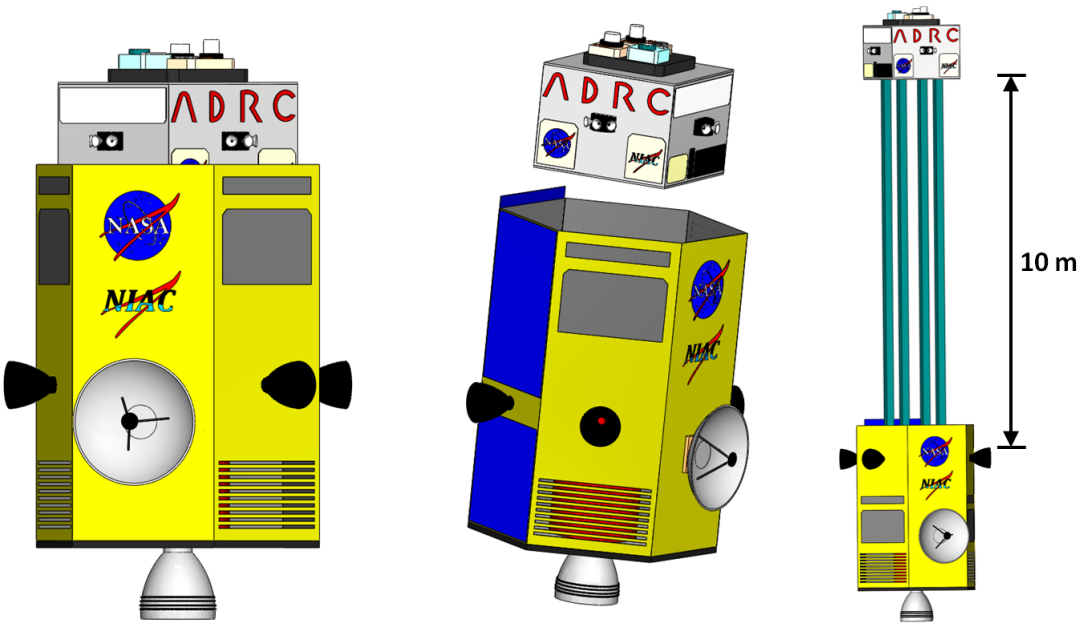

(a) Primary stowed (b) Primary separated (c) Optional boom

Figure 2: The primary and optional two-body HNIS configuration during the terminal phase.

with respect to the target, signal processing and logic, and an output circuit to initiate firing.[12] Without the proper selection of a reliable triggering or fuzing mechanism, there is a high risk that the mission can be unsuccessful. Current terrestrial triggering systems such as salvage fuzes, timing, contact, and radar (proximity) fuzes are employed to detonate the NEDs. These fuzes act on the instantaneous scale between 10 - 25 microseconds. This allows for absolute precision required for a hypervelocity impact nuclear disruption mission.

The salvage fuze acts as a contingency fuze which is employed as a failsafe detonation. The fuze "salvages" the bomb and explodes when all other fuzes fail.[11] The salvage fuze serves as a countermeasure to a terminal defense interceptor system and initiates after a detected collision possibility. The warhead then explodes as soon as an interceptor comes within a certain range of the warhead. Sometimes radar and contact fuzes operate as the failsafe triggers and must function after withstanding extreme deceleration forces and delivery vehicle deformation.[11] In an asteroid direct intercept scenario, the salvage fuze comprised of several contact and radar fuzes becomes activated. The contact and radar fuzes provide one option for arming and detonating the NED.

Another option for triggering the NED is a timing fuze. The timing fuze operates by using time-to-go, estimated intercept distance, and the rate of the intercept distance. This information is provided to the triggering mechanism by the guidance, navigation, and control instruments and flight computer. The computer activates the timing fuze once the guidance parameters meet specific conditions. The timing fuze is the most appropriate as the entire deflection/disruption process will be autonomous. However, if the timing fuze proves to be inaccurate, the salvage fuzes (contact and radar fuzes) can restore the arming mechanism of the NED. A salvage fuze is always present to resume the arming of the NED in any such triggering problems.

Proper fuzing systems and operations need to be chosen. For a standoff burst disruption mission,

Table 1: HNIS Imaging sensor package properties.

Parameter	NFOV Imager	WFOV Imager
Field of View (deg)	2.3 × 2.3	9.5 × 9.5
Angular Resolution (μrad)	10	40
Focal Plane Dimension (pixels)	1024 × 1024	1024 × 1024
Effective Aperture Size (cm)	8.5	2.1
Effective Focal Length (cm)	90	22.3
Estimated Mass (kg)	15	10
Estimated Power (W)	20	10

radar acts as part of the primary fuzing system. For the subsurface or contact burst option, timing and radar fuzes may represent part of the primary detonation system, and contact fuzes are used as a failsafe detonation. The selection and sequencing of these fuzing options are chosen autonomously and are not dependent on additional hardware or configurations. Contact and radar fuzes can be located on top (front) of the follower spacecraft and in the thermal shield. However, the timing fuze and NED remain protected by the thermal shield.

Terminal Guidance Sensors/Instruments

Optical cameras, radar altimeters, and Light Detection and Ranging (LIDAR) are used on the leader spacecraft to accurately identify and track the target NEO and initiate fuzing for the NED. The leader uses a Medium Resolution Instrument (MRI) or Wide Field of View (WFOV) Imager as used on the Deep Impact flyby spacecraft. The WFOV Imager is used to locate the target NEO at the start of the terminal phase. It is a small telescope with a diameter of 12 cm and takes images with a scale of 10 m/pixel in a spectrum of approximately 700 km.[8] The field of view of the WFOV Imager is approximately 10 deg x 10 deg which allows to observe more stars and serves as a better navigator for the HNIS during its coasting phase.[8] As soon as possible after acquisition of the target NEO, the WFOV Imager passes information to the High Resolution Instrument (HRI) or Narrow Field of View (NFOV) Imager, which has a field of view of 2.3 deg x 2.3 deg. It is comprised of a 30-cm diameter telescope that delivers light to both an infrared spectrometer and a multispectral camera. The camera has the ability to image the NEO with a scale that is less than 2 m/pixel when the spacecraft is approximately 700 km away.[8] Table 1 shows the properties of each Imager. The Imagers are located on the leading front of the impactor spacecraft. These Imagers are similar to the instruments used on the Deep Impact Mission Flyby and Impactor spacecraft.

LIDAR or laser radar measures back-scattered light from a high intensity, short duration output pulse transmitted at the target NEO. It is used in the closing minutes of the terminal phase to calculate the range to the NEO. This information is shared with the fuzing device for detonation of the NED. The LIDAR requires sufficient power to operate over a range equivalent to approximately the last minutes of the terminal phase. The device design would be similar to the ones used on the NEAR and Clementine missions. The LIDAR has a mass of 20 kg and an estimated power consumption of 50 W. Radar altimeters using radio waves are used in conjunction with LIDAR.

Thermal Protection and Shield

An in-house hydrodynamics code, which is being developed to accurately study the effects of nuclear disruption missions, is used to estimate the thermal and structural limits experienced by the

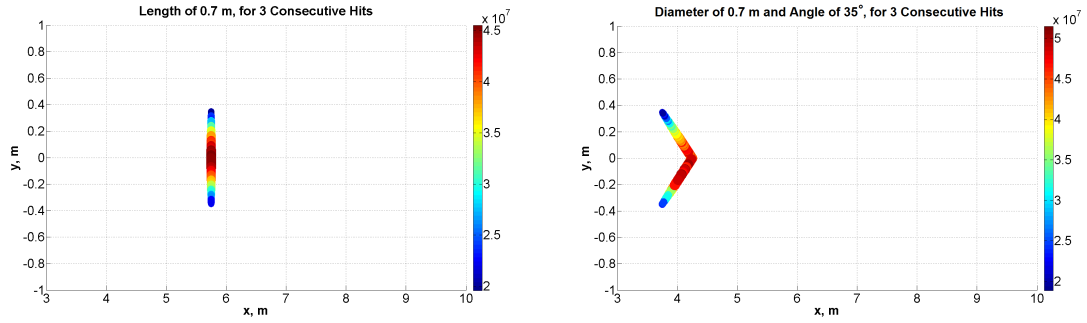

(a) A flat plate.

(b) A conical cone.

Figure 3: Estimated penetration depth of a flat plate and conical cone based on 3 consecutive hits at the same location.

two-body HNIS. The hydrodynamic code helps to establish a shield design and its configuration on the follower spacecraft. Several different geometries include a flat cylindrical plate, conical shape, spherical cap, and an EPW ogive nose cone.

Due to long turnaround times inherent to the use of any hydrocode for testing different shield designs and material properties, a single energy simulation of the impact event was ran and saved. The simulation starts with a spherical leader spacecraft impacting an asteroid modeled with strength properties of granite. The leader spacecraft traveling at approximately 10 km/s is vaporized at impact. Approximately 1 microsecond later, the follower spacecraft impacts the same location as the leader spacecraft. The energy experienced by the follower spacecraft is recorded and the simulation is saved. The simulation variables are then used in a MATLAB simulation code to observe energy interactions for given shield geometries. Once the MATLAB shield test concludes specific geometries, the hydrocode simulation tests shield geometry, material properties, and shield thickness. Dissipating energy from the shield is not considered at this time but will be included in future work.

Figures 3-4 show the energy interaction for a MATLAB simulation using different geometries (thin flat plate, cone, spherical cap, and an ogive nose cone). The simulation has 36 time steps with the shield starting point at approximately 10 m from the asteroid and the ending point at a subsurface depth of 17 m. Each shield is geometrically different but the same mesh size of 5,000 points is used. The color bar legend on the right hand side of each figure shows the amount of energy encountered by the shield. It is shown that the reddest areas located on the shield confronted the highest amounts of energy (usually in the center of the shield). One study is presented using the same simple MATLAB simulation test. The simulation was stopped when a location on the shield was consecutively hit 3 times with the largest amount of energy. Figures 3-4 show the location of the shield at a subsurface depth in the asteroid and the highest amount of energy endured by the shield. From these early simulations, we can infer a shield length and geometry that can be tested in the hydrodynamics code.

Once the geometry of a shield is chosen, the mass can be estimated. A list of materials used for thermal resistant shielding in space missions are considered and listed in Table 2.[15] Because of the hypervelocity impact of the HNIS, the heat of vaporization is the major concern. As the leader spacecraft of HNIS impacts, material composition on the asteroid and the materials on the

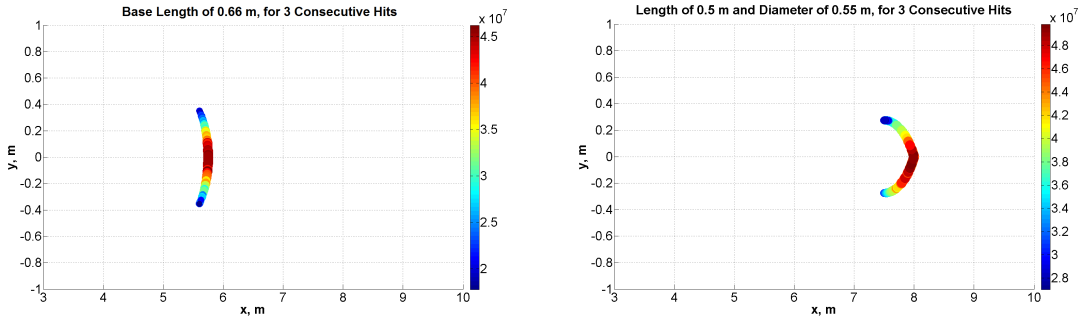

(a) A spherical cap.

(b) An ogive nose cone.

Figure 4: Estimated penetration depth of a spherical cap and ogive nose cone based on 3 consecutive hits at the same location.

Table 2: List of materials and their properties considered for a thermal shield.

Materials	**Density (kg/m^3)**	**Energy to Melt (J/kg)**	**Energy to Boil (J/kg)**	**Energy to Vaporize (J/kg)**
Aluminium	2,700	8.40e5	2.47e6	1.1e7
Beryllium	1,848	2.82e6	5.9e6	3.3e7
Cadium	8,650	1.37e5	2.39e5	8.88e5
Copper	8,960	5.3e5	1.1e6	4.73e6
Iron	7,874	7.96e5	1.33e6	6.26e6
Magnesium	1,738	9.41e5	1.39e6	5.24e6
Niobium	8,570	7.15e5	1.30e6	7.43e6
Silicon	2,330	1.2e6	2.51e6	1.28e7
Titanium	4,500	1.08e6	1.98e6	8.88e6
Tungsten	19,250	4.80e5	7.57e5	4.48e6
Vanadium	6,100	1.07e6	1.80e6	8.87e6
Zirconium	6,520	5.73e5	1.26e6	6.47e6

follower spacecraft of HNIS act like liquid plasma, vaporizing as they both collide with the target asteroid. To make certain of the survivability of the NED and its triggering system, a mass-efficient and thermal resistant material is needed. From Table 2, it can be seen that aluminum, beryllium, and silicon require very high energy to vaporize. A large variety of alloys are readily available with aluminum providing moderate temperature and good strength-to-weight ratio. Beryllium offers the highest stiffness with high temperature tolerance but its toxicity to humans requires extensive safety measures.[15] Silicon is usually mixed with other metals to provide more strength and higher thermal tolerances. Mixing it with carbon creates a great protective covering used in space mission applications such as the space shuttle. Also, titanium is a lightweight, high strength metal that can endure extreme temperatures but lacks durability. A thorough analysis of structural loads and thermal loads is undertaken through the ADRC's hydrodynamics code to find the best material properties for the thermal shield.

The hydrodynamics code developed by the ADRC is based on a meshless model used previously for asteroid impactor analysis.[13] The initial impact is generated by a spherical shell matching the

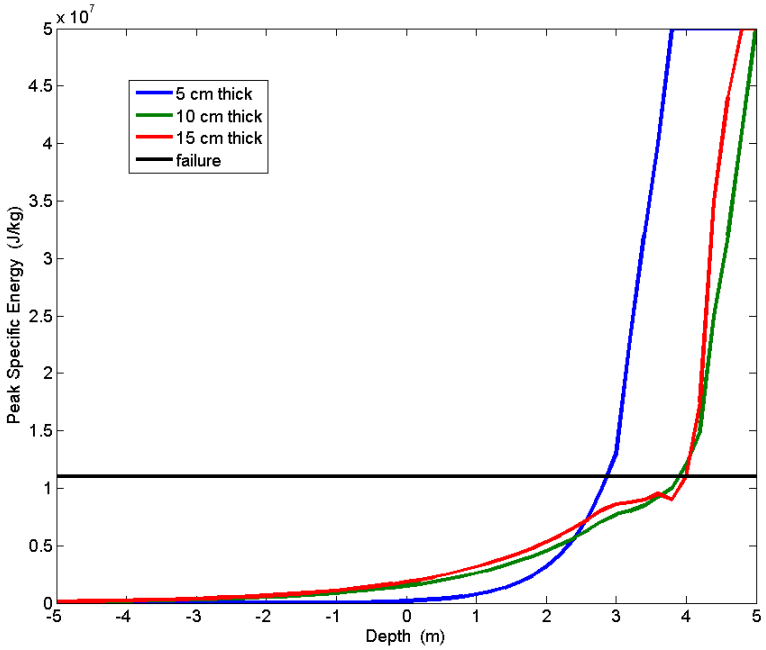

Figure 5: Peak payload specific energy for flat shield design.

mass of the leading body, resulting in a field of hot gas and ejecta through which the payload must survive. It is suggested in Reference 14 that most warhead designs will experience melting or exceed the maximum allowable structural load in this region. Therefore, a shield design is desirable to mitigate the effects of incident vaporized rock from the lead body, substantially protect the payload from micrometeorites ejected from the impact, and allow for the maximum depth of burst. Figure 5 shows the peak specific energy of a 0.7 m diameter cylindrical aluminum payload shield as a function of depth for three nominal thicknesses. The horizontal line represents failure of the system to adequately protect the payload, resulting in failsafe detonation.

As observed in Figure 5, a minimal thickness for this shield is about 10 cm. Above this value, little additional penetration is observed, given the thermal gradient in this region. A complicating factor is the acceleration of the payload. The 10 km/s initial relative speed greatly exceeds the speed of sound in the shield structure, resulting in the equivalent of a standing shock along the shield. Ahead of this shock, the payload measures only minimal interruption. Some initial acceleration due to ejecta impacts and interaction with the gas environment is measurable, but shortly thereafter the maximum structural load is reached. An example estimate of peak acceleration as a function of depth for the previously discussed shield is found in Figure 6. Thickness of the shield has almost no effect on the maximum depth reached before structural failure, making overly thick shields a hindrance rather than a benefit.

Since the acceleration of the payload is almost discontinuous as it approaches the impact shock, a successful fuzing system must address this by timing detonation as a result of measurable information. This will either require sensors and triggers capable of reacting to the observable impact precursors (on the order of 10-20 microseconds), or more likely will require an array of sensors placed ahead of the payload. This could be accomplished either by placing sensors within the shield, or at the top of the follower spacecraft. A challenge to this approach would be that the

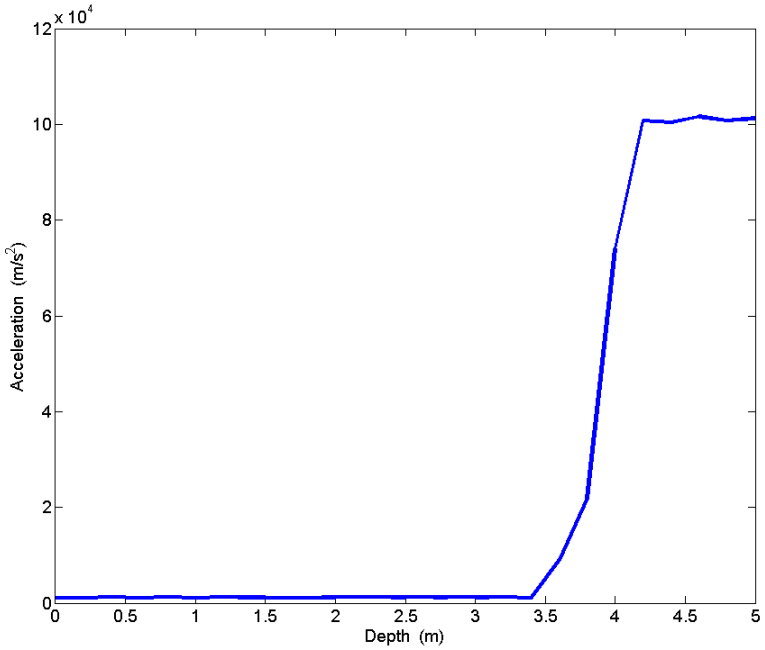

Figure 6: Example acceleration measurements for flat shield design.

Table 3: DOB based on thickness parameter and shield geometry.

Shield	Thickness (cm)	Mass (kg)	DOB (m)
Flat Cylinder	9.4	97.7	3.8
Conical	10.1	105.0	4.1
Spherical	8.8	76.8	5.3
Ogive	10.5	116.1	4.6

sensors would need to survive in an environment capable of vaporizing many metals at least long enough to trigger the payload before impact.

Table 3 shows the results for minimum thicknesses and masses (of aluminum) of the flat, conical, spherical, and ogive nose cone discussed previously. These thicknesses are chosen to allow survival of the payload until the shield experiences structural failure. Further study found these thicknesses to depend very little on the material chosen, other than the mass of the resulting system, as the shape of the shield and the leader spacecraft tend to govern the achievable depth. Also listed in Table 3 is the maximum achieved depth of burst (DOB). Reduced performance can be achieved by using thinner shields, and lowering the required DOB would result in benefits for timing the detonation of the payload.

Based on this initial study, few conclusions can be drawn for the design of the payload thermal shield. First, the primary variables in achievable DOB is the shape, mass, and timing of the leader spacecraft. Additional analysis must be done to optimize this portion of the mission. Second, given a particular environment, a discontinuous shock to the payload presents challenges in determining how far to allow penetration before detonation. The payload cannot survive a direct impact at this speed, so it must be triggered using a combination of sensor and optical data at an appropriate data

rate. Third, geometry of the shield seems to present a greater influence on DOB than any other variable. Adding thickness to the thermal shield in excess of the minimums presented do not result in further penetration, since both shields experience high structural loads at the maximum DOB. Finally, these results appear to be independent of the materials tested, as the limiting factor is the acceptable structural loads on the payload. However, significant mass can be saved by utilizing lighter alloys or materials for the thermal shield.

Optional HNIS Configuration Employing Deployable Booms

The leader and the follower can be separated and connected by deployable booms to ensure the NED payload follows the leader spacecraft safely and reliably. The boom must be sufficiently rigid to avoid oscillation motion of the two bodies. A deployable mechanism is preferable compared to a fixed structure due to volume constraints in the launch vehicle fairing. The connection mechanism can be divided into four categories, hinged, telescoping, an articulated mast system, and carbon fiber reinforced plastics (CFRP).

A hinged deployable boom consists of a hinged truss structure that is collapsible in storage and when deployed, locks into place and is held firm. ATK, the manufacturer of such trusses, reports 12.4 m and 6.2 m length trusses both with bending stiffness of 1.5×10^6 N·m^2, although mechanical properties are dependent on component materials.[18] Depending on the materials of the components for the system, the mass cost of such a system could be high. Most such trusses are planned to be retractable which adds a level of complexity that is unnecessary for the HNIS application. ATK has manufactured many systems that have been tailored to specific mission requirements, and provides a favorable flight history. Another option that can also be classified as a hinged deployable boom is the folding hinged boom. ESA has been developing such systems and are much like the hinged truss. This particular option does not have the flight history as reported by ATK but mostly because it is highly tailorable to each application, making comparison difficult. The mass and mechanical properties of the hinged booms are strongly tied to the material selected. Composite materials may be lighter but more expensive and metals would be heavier but easier to manufacture.

ATK also provides a telescoping system which is also meant to be retractable. ATK reports a 5.5 m (deployed) boom with a bending strength of 72,000 N that weighs 20 kg.[18] Unfortunately, when the boom is deployed, the diameter of the next telescoping section is reduced in order to be efficiently stored. This option has a high mass cost and is used primarily for larger spacecraft applications.

The articulated mast system is designed and manufactured by ATK and is used for deploying critical spacecraft payloads. It can be tailored for specific mission requirements and has efficient stowage volume. Its deployment capability has a high push force with or without active controls. It has lengths up to 60 m with a bending load capacity of 8,100 N·m and a bending stiffness of 5.76×10^8 N·m^2. The articulated mast system has had successful deployment on multiple ISS/STS missions.[18] Figure 7a shows the articulated mast system in its stored and deployed state.

Solar sails have previously employed deployable booms made of carbon fiber reinforced plastics (CFRP). The booms (which can be made up to 20 m) have a cross section shown in Figure 7c. When the cross section is flattened, by pulling horizontally, the material can be coiled as illustrated in Figure 7b. The CFRP wraps in an "S" coil which occupies more volume than anticipated. The dimensions of the structure is designed to fit specific loads. There are also similar models that are pressurized (inflatable) to increase strength and stiffness. According to Reference 17, a 14-m boom

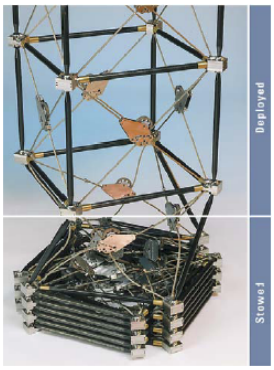

(a) Articulated mast system stowed and deployed.

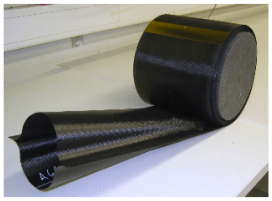

(b) CFRP Coiled

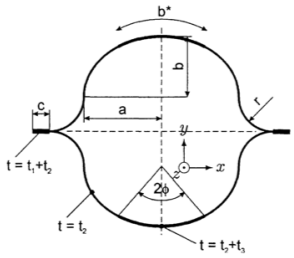

(c) CFRP Cross Section

Figure 7: Illustrations of the different boom options that can be employed for the HNIS.

has a bending stiffness of approximately 5,200 N·m^2. More research is needed to choose the boom that meets the requirements of connecting the two bodies of the HNIS.

Shock Prevention Systems

A shock prevention system may be needed to protect the NED and the triggering mechanisms from the structural shock upon impact. Hypervelocity testing is difficult and expensive making hypervelocity protection system technology premature. Nonetheless, further study of current shock prevention systems can provide a starting place for a hypervelocity nuclear interceptor application. Current shock prevention systems include airbags (automobiles and spacecraft landing systems), steel and foam energy reduction barriers, hydraulic isolators and dashpots, and foam and fiber-matrix material systems.

Airbags have been used extensively in automobiles as a safety device. It consists of a flexible shape designed to inflate instantaneously during an automobile collision. It's purpose is to prevent occupants from striking interior objects. Airbags are also used in aerospace applications, in particular, the landing of the Mars Pathfinder exploration rover to dissipate the impact energy upon landing. The airbag configuration inflates and absorbs the impact shock when the rover is traveling less than 25 m/s. These airbags (90 kg) are rated for a maximum of 50 g deceleration for the 290 kg rover.[16] The material of the airbag and the pressure inside the airbag can be chosen depending on the kinetic energy of the object. However, airbags perform efficiently at lower speed levels and might prove to be ineffective for dissipating energy for a hypervelocity impact.

The steel and foam energy reduction barriers or soft walls are found in competitive racing. Other forms of soft walls include cello foam (mixture of polystyrene and polyethylene barriers), polyethylene energy dissipation system (stacked polyethylene cylinders), and rubber casings tied to concrete walls. Soft walls provide safer accidents in place of concrete barriers and less destructive damage to the race car on impact. The steel and foam energy reduction barriers consist of structural steel tubes and bundles of closed-cell polystyrene foam. The theory behind the design is that the barrier absorbs a small amount of the kinetic energy which is dissipated along the wall, rather than transferred back into the impacting object. Different types of density foams amounts to the energy that can be absorbed from an impact. Foam thickness, firmness, density, and porosity may affect how well the foam system can absorb shock (impact dissipation) and decelerate an object. Foams with

the lowest porosity are generally better suited foams for heavier objects requiring greater energy absorption.[17] The energy dissipation comes from the distortion of the material, however the energy levels of a hypervelocity impact coincide with the vaporization of most materials. Even if the foam were to survive, the amount of energy absorption required would be so large that the volume and mass of the system would be infeasible. Hydraulic isolators, dashpots, dampers, and buffers are primarily used for shock and vibration prevention during storage and launch of aerospace and defense applications. Currently, a shock prevention system capable of handling the impact energy does not exist. Experimental efforts and testing of an integrated shock prevention system could be required for hypervelocity impacts.

Attitude Determination and Control System (ADCS)

A baseline ADCS of the HNIS is modeled after the flight-proven system of the Deep Impact mission[20] with minor adjustments for the specific purposes of the HNIS. A baseline Divert and Attitude Control System (DACS) of the HNIS consists of 4 large divert thrusters each capable of 540 N of thrust using monomethylhydrazine (MMH) fuel and multiple smaller thrusters producing 30 N of thrust. The 4 large divert thrusters are positioned at the center of mass to provide two-directional translational control during the terminal guidance phase. The smaller thrusters are used to change and maintain the attitude of the spacecraft. The total number of thrusters and their specific locations on each spacecraft need to be further studied.

The sensors of the baseline ADCS include one Northrop Grumman Scalable Space Inertial Reference Unit (SSIRU), four Ball Aerospace's CT-633 Star Trackers, and one Imager. The SSIRU contains four Hemispherical Resonator Gyro Sensors and four accelerometers which provide a reading of angular rates and accelerations of the body in the body frame. The star trackers provide quaternions of the boresight of the instrument which then can be used to calculate attitude of the spacecraft.[21] The Imager acquires images of the impact site which are then processed for both trajectory and attitude adjustments.[22] The attitude is controlled by a set of small thrusters.

The ADCS has three operational modes, De-Tumble, Approach, and Impact. The De-Tumble mode occurs at the beginning of the terminal phase and is meant to stabilize the spacecraft's attitude. During the Approach mode, the ADCS maintains attitude while GNC executes maneuvers to impact the target NEO. During the Impact mode, ADCS gives attitude adjustments in preparations for terminal impact. Precision attitude stabilization of the two bodies, connected by deployable booms, can be a challenging control problem. In addition to the stated modes, ADCS also needs a safe mode that is required if the spacecraft is malfunctioning or experiencing unexpected errors. If this safe mode is activated, it will place the spacecraft into a low rate stabilizing spin until errors can be addressed.

Power System

The peak power usage estimates for the baseline HNIS are listed in Table 4. Mode 1 is the initial phase of the mission and occurs immediately after spacecraft deployment from the launch vehicle fairing. During this mode, the spacecraft is performing all check-out operations and de-tumble maneuvers. Communications remain off until the attitude of the spacecraft is stabilized. Mode 2 is the main mode that the spacecraft remains in during the transfer phase and interval parts of the terminal phase. Mode 3 is used for deep space maneuvers and TCMs during the orbit transfer phase. Through these periods, the communications and thermal controls are briefly suspended to save power. Mode 4 is the final phase for both the leader and the follower spacecraft. As power for

Table 4: Peak power budget of each subsystem of the HNIS in various operational modes.

Types of Mission Phase and Power Mode				
	Departure	Orbit Transfer	TCMs	Terminal Phase
Subsystem	**Mode 1**	**Mode 2**	**Mode 3**	**Mode 4**
Propulsion	180	0	180	0
Command and Data Handling	70	70	70	70
Electrical Power	50	50	50	50
Telecommunications	0	220	0	220
Guidance, Navigation and Control	80	0	80	80
Attitude Determination and Control	75	0	75	75
Thermal Control	60	60	0	0
NED Payload	0	0	0	15
Subtotal (W)	**515**	**400**	**455**	**510**
20% Margin	103	80	91	102
Total Power(W)	**618**	**480**	**546**	**612**

targeting, communications, and trajectory adjustments rise, the thermal control system's power is reduced. It should be noted that the power requirement for arming the NED in mode 4 is applicable for the follower spacecraft. As the operations of the HNIS are refined for each specific disruption technique, more accurate peak power estimates can be achieved.

During the orbit transfer phase, solar cells along with secondary batteries can be used. For the maximum peak power required during transfer, a minimum area of 3.3 m^2 is needed. A 7.4 m^2 Emcore InGaP/InGaAs/Ge triple-junction solar cell panel with greater than 30% cell efficiency is mounted on one entire face of the spacecraft. It is intended that this face will be in nearly direct sunlight throughout the duration of the mission. Two adjacent faces also have solar cells. These three arrays will produce sufficient power for recharging secondary batteries after peak operations. Secondary rechargeable batteries will be necessary to power the spacecraft during peak and non-peak power operations. Research in this area is still needed to ensure the optimal product for the operations. Since secondary batteries are rechargeable, the mass of these batteries is much smaller. The follower spacecraft can use 2 Lithium-ion rechargeable batteries, each with a mass of 6 kg and capable of 300 W·h with an approximate time to recharge of 40 minutes.[15] Similar batteries have been used on the Mars Spirit and Opportunity Rovers.

Since the terminal phase requires a sufficient amount of power for at least 24 hours, the leader and follower spacecraft use primary batteries. Silver-cadmium and Nickel type batteries have a high mass cost due to their low-energy densities for the required 24-hr period. Although Silver Zinc has had a long flight history, the mass cost of such a battery is still higher than that of a Lithium type battery.[15] A Lithium type battery has a very high energy density such that for an intensive power period of 24 hours, the Lithium type batteries have an estimated mass of 17 - 43 kg.[15]

Mass Budget Summary

Table 5 shows the mass breakdown of a baseline primary HNIS carrying a 1000-kg NED payload. The leader spacecraft has a wet mass of 315 kg and the ability to provide a total ΔV of 270 m/s which is similar to what the impactor spacecraft used in the Deep Impact mission during its terminal phase. The follower spacecraft has a dry mass of 1,170 kg carrying an NED payload of 1,000

Table 5: Mass breakdown for a baseline primary HNIS using Delta IV M+ launch vehicle class.

Vehicle	Description	Mass (kg)
Leader/Impactor	Dry Mass	285
	MMH Propellant	30
	Wet Mass	**315**
Follower	Dry Mass	1,170
	NED Payload	1,000
	Thermal Shield	135
	Deployable Boom (Optional)	55
	Total Dry Mass	**2,170**
	N_2O_4 Propellant	775
	Wet Mass	**2,945**
Total Spacecraft	Dry Mass	2,455
	Wet Mass at Launch	3,260
	Mass at NEO	2,710
	Mass Margin (30%)	978
	Total Mass w/ Margin	**4,238**

kg. Depending on the material selected, the thermal shield and the optional deployable booms are estimated at an average of 135 kg and 55 kg, respectively, which correspond to previous space missions (Deep Impact Mission and Space Shuttle). The follower spacecraft also has the propellant necessary to execute trajectory correction maneuvers (ΔV of 550 m/s) during the transfer orbit and adjustment maneuvers (ΔV of 270 m/s) during the terminal phase. The mass of the HNIS upon arrival at the target NEO is estimated at 2,710 kg. A mass margin of 30% is used to account for uncertainties, thus making the total wet mass at launch approximately 4,238 kg.

Figure 8a illustrates the HNIS in a Delta IV M+ fairing. Without using an upper stage or orbital transfer vehicle, the Delta IV M+ has the capability to deliver the HNIS in a direct C3 trajectory towards the target NEO.[23] The propellant system on the HNIS uses a bi-propellant feed system of dinitrogen tetroxide (N_2O_4) coupled with MMH attitude thrusters. The N_2O_4 propellant system has a restartable engine capable of producing 4,400 N of thrust at a specific impulse of 326 seconds, making it favorable for executing TCMs. The MMH attitude thrusters are used for attitude adjustments and terminal adjustment maneuvers. The leader and follower spacecraft are equipped with small MMH attitude thrusters.

The proposed HNIS, as shown in Figure 8b, takes the form of a box-shaped impactor spacecraft equipped with thrusters and targeting instruments. It connects to a hexagon-shaped follower spacecraft equipped with 4 divert thrusters, a high-gain antenna, a thermally resistant shield, and an NED. The HNIS has a total length of approximately 6.7 m and a circular base of 4 m. The follower spacecraft incorporates a shelf that holds the leader spacecraft and the optional stowed booms. The leader spacecraft separates from the follower spacecraft by pyrotechnic attachments.

The HNIS is configured by using unscaled dimensions of commercial off-the-shelf components and materials such as ATK's fuel tanks, bi-propellant engine, optical instruments, etc. These dimensions and mass properties accurately reflect a preliminary configuration of an innovative HNIS. Through these dimensions and mass properties, the center of mass (COM) can be calculated. The reference coordinate system lies at the top center of the engine with the y-axis going through the

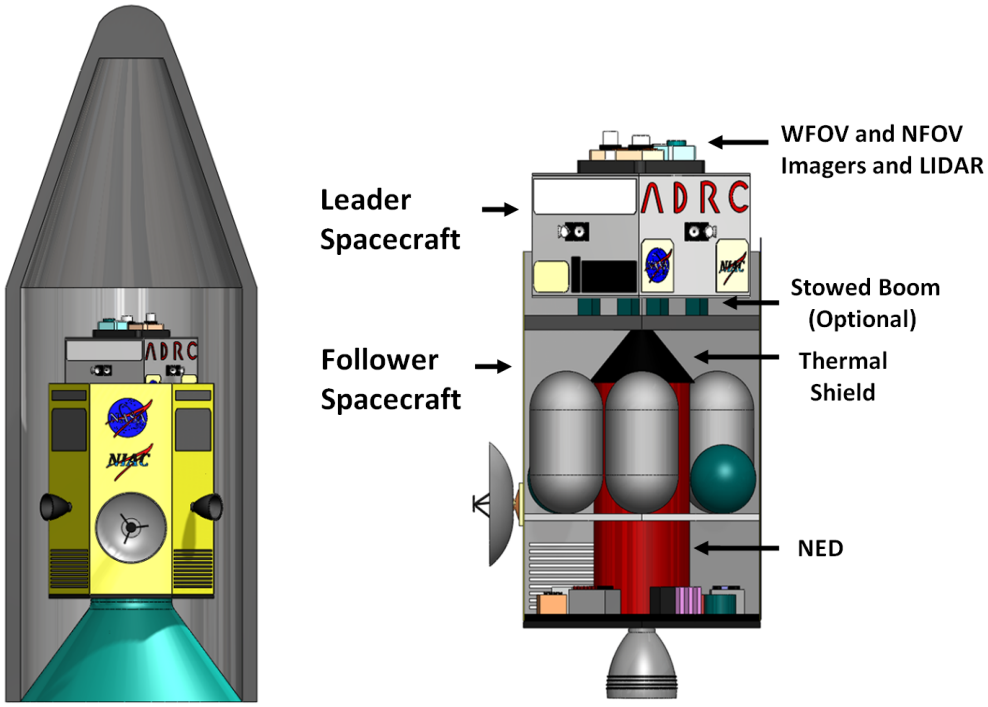

(a) (b)

Figure 8: A baseline two-body HNIS configured for launch.

length of the spacecraft, the z-axis pointing away from the HGA, and the x-axis orthogonal to both. Assuming the COM of each component is its centroid, the COM of the HNIS at launch is located at (0, 2.15, -0.013) m. After separation between the two bodies, the follower spacecraft takes on a new COM at (0, 1.8, -0.018) m. The divert thrusters are pre-positioned at this new y_{COM} component as depicted in Figure 8a. If the optional configuration of the HNIS with a rigid boom connection between the two bodies is chosen, the COM moves along the y direction towards the top front of the follower spacecraft. A 10-m rigid boom connecting the two bodies yields a new COM at (0, 3.45, -0.016) m. However, a 16.5-m boom could be used producing a y_{COM} of 4.22 m but is not advised as the length of the follower spacecraft is 4.3 m. The leader and boom shelf is located at 3.6 m and serves as a conservative location to not allow the COM to go beyond. By constraining the COM to the boom shelf or below, a 10-m rigid boom can be used.

Other secondary concept options of the HNIS exist depending on ΔV demand, mission budget, and NEO characteristics. NED payloads and fuel tanks can be interchanged easily with slight modification to the HNIS and to accommodate different launch vehicles. A Delta II class launch vehicle in conjunction with an upper stage can be used to launch a smaller HNIS (1,450-kg) that is capable of carrying a 300-kg NED payload. Likewise, a Delta IV Heavy launch vehicle class can deliver a scaled up version of the HNIS (3,770-kg) able to carry a 1,500-kg NED payload. According to Reference 23, the total mission costs to launch an HNIS (without NED payloads) by a Delta II, Delta IV Medium, and Delta IV Heavy launch vehicle are estimated as approximately $490M, $1,076M, and $1,274M, respectively. While such a demo mission will not involve an NED, it will prove the fusing capability, and the kinetic impact will provide experimental information on the asteroid's response

to the sharp impulse of an impactor or an NED.

CONCLUSION

When the warning time of an Earth-impacting asteroid is short, the use of nuclear explosives may become necessary to optimally disrupt the target NEO. Requirements of a nuclear disruption mission prove to be challenging due to direct intercept speeds, nuclear disruption technique, impact speed limit of state-of-the-art NED fuzing mechanisms, and structural and thermal loads acting on the spacecraft. A concept of blending a hypervelocity kinetic impactor with a subsurface nuclear explosion has been proposed for optimal penetration, fragmentation, and dispersion of the target NEO. A baseline hypervelocity nuclear interceptor system consists of a kinetic-impact leader spacecraft and a follower spacecraft carrying a 1,000 kg-NED. A preliminary development of an HNIS, including thermal shielding simulations, selection of fuzes and optical instruments, terminal guidance operations, and other secondary configurations have been discussed in this paper. A more detailed spacecraft subsystem design is needed to prove spacecraft feasibility and durability. Additional hydrodynamic simulations include unique hypervelocity impact shields, calculation of the optimal separation distance between the two-body system, and possible illustration of the terminal phase for each nuclear disruption technique.

ACKNOWLEDGMENT

This study was supported by the NIAC (NASA Innovative Advanced Concept) Phase 1 program of the NASA Office of the Chief Technologist. The authors would like to thank Dr. John (Jay) Falker, the NIAC Program Executive, for his support of this research project. Dr. David Dearborn works under the auspices of the US Department of Energy at Lawrence Livermore National Laboratory under contract DE-AC52-07NA2734. Special thanks also go to research assistants Kevin Doetsch and Elizabeth Gregory working at the ADRC for their supportive research efforts.

REFERENCES

[1] B. Wie, "Hypervelocity Nuclear Interceptors for Asteroid Deflection or Disruption," *IAA 2011 Planetary Defense Conference*, Bucharest, Romania, 9-12 May 2011.

[2] *Defending Planet Earth: Near-Earth Object Surveys and Hazard Mitigation Strategies: Final Report*, National Research Council, 2010. nap.edu/catalog/12842.html

[3] B. Wie, and D. Dearborn, "Earth-Impact Modeling and Analysis of a Near-Earth Object Fragmented and Dispersed by Nuclear Subsurface Explosions," AAS 10-137, AAS/AIAA Space Flight Mechanics Meeting, 2010.

[4] S. Wagner, A. Pitz, D. Zimmerman, and B. Wie, "Interplanetary Ballistic Missile (IPBM) System Architecture Design for Near-Earth Object Threat Mitigation," *2009 International Astronautical Congress*, Daejeon, Korea, 2009.

[5] *Effects of Nuclear Earth-Penetrator and Other Weapons*, National Research Council, 2005. nap.edu/catalog/12842.html

[6] B. Kaplinger, B. Wie, D. Dearborn, "Preliminary Results for High-Fidelity Modeling and Simulation of Orbital Dispersion of Asteroids Disrupted by Nuclear Explosives," AIAA-2010-7982, AIAA Guidance, Navigation, and Control Conference, 2010.

[7] A. Pitz, C. Teubert, B. Wie, "Earth-Impact Probability Computation of Disrupted Asteroid Fragments Using GAMT/STK/CODES," AAS-2011-408, AAS/AIAA Astrodynamics Specialist Conference Girdwood, AK, 2011.

[8] D. Kubitschek,"Impactor Spacecraft Encounter Sequence Design for the Deep Impact Mission," Deep Space Systems, 2008.

[9] "ESA - NEO Don Quijote Concept," European Space Agency, 2005. esa.int/esa.html

[10] I. Carnelli, A. Galvex, F. Ongaro, "Industrial Design of the Don Quijote Mission," *57th International Astronautical Congress*, 2006.

[11] C. Hansen, "Part V: Arming and Fuzing: Techniques and Equipment," 1995. cryptome.org/nuke_fuze.htm

[12] "Nuclear Weapon Design," Federation of American Scientists, 1995. fas.org/nuke/design.htm

[13] B. Kaplinger, B. Wie, and D. Dearborn, "Nuclear Fragmentation/Dispersion Modeling and Simulation of Hazardous Near-Earth Objects," IAA Planetary Defense Conference, Bucharest, Romania, May 9-12, 2011.

[14] V. G. Chistov et al., "Nuclear Explosive Deep Penetration Method into Asteroid," Central Institute of Physics and Technology, Russia, 1997. csc.ac.ru/news/1997_1/ae31.pdf

[15] J. French and M. Griffin, *Space Vehicle Design*, AIAA, 2004.

[16] "Mars Pathfinder and Mars Rover Airbag Systems," ILC Dover, 2011. ilcdover.com/Mars-Pathfinder-Exploration-Rover-MER/

[17] "Information on Flexible Polyurethane Foam," Polyurethane Foam Association, INTOUCH, Vol. 5, 1996.

[18] "Deployable Structures," ATK, 2011. atk.com/capabilities/deployable_structures.asp

[19] L. Herbeck et al., "Development and Test of Deployable Ultralightweight CFRP-Booms for a Solar Sail," European Conference on Spacecraft Structures, Materials and Mechanical Testing, 2000.

[20] M. Hughes, C. Schira, "Deep Impact Attitude Estimator Design and Flight Performance," *Advances in Aeronautical Sciences,* Published for the American Astronautical Society by Univelt, 2006.

[21] "Space Inertial Reference Units," Northrop Grumman, 2011. es.northropgrumman.com/solutions/siru/

[22] D. Kubitschek et al., "Autonomous Navigation for the Deep Impact Mission Encounter with Comet Tempel 1," Deep Impact Mission: Looking Beneath the Surface of a Cometary Nucleus, 2005.

[23] G. Vardaxis et al., "Conceptual Design and Analysis of Planetary Defense Technology Demonstration Mission," AAS 12-128, AAS/AIAA Space Flight Mechanics Meeting, 2012.